Pramana – J. Phys. (2019) 92:18
https://doi.org/10.1007/s12043-018-1683-1

A reliable algorithm for fractional Bloch model arising in magnetic resonance imaging

AMIT PRAKASH[1,*], MANISH GOYAL[2] and SHIVANGI GUPTA[2]

[1]Department of Mathematics, National Institute of Technology, Kurukshetra 136 119, India
[2]Department of Mathematics, Institute of Applied Sciences and Humanities, GLA University, Mathura 281 406, India
*Corresponding author. E-mail: amitmath@nitkkr.ac.in, amitmath0185@gmail.com

MS received 7 May 2018; revised 13 June 2018; accepted 26 June 2018; published online 2 January 2019

Abstract. Magnetic resonance imaging (MRI) is used in physics, chemistry, engineering and medicine to study complex materials. In this paper, numerical solution of fractional Bloch equations in MRI is obtained using fractional variation iteration method (FVIM) and fractional homotopy perturbation transform method (FHPTM). Sufficient conditions for the convergence of FVIM and its error estimate are established. The obtained results are compared with the existing as well as recently developed methods and with the exact solution. The obtained numerical results for different fractional values of time derivative are discussed with the help of figures and tables. Figures are drawn using the Maple package. Test examples are provided to illustrate the accuracy and competency of the proposed schemes.

Keywords. Fractional model of Bloch equations; fractional variation iteration method; magnetic resonance imaging; Caputo fractional derivative; fractional homotopy perturbation transform method.

PACS Nos 76.60.−k; 87.19.Lf; 87.10.Ed; 02.60.Cb

1. Introduction

Initial references to derivatives of fractional order were made in the 17th century. In the past few decades, fractional-order calculus has emerged as a potential tool in various domains of science and engineering such as fluid dynamic traffic [1], neurophysiology [2,3], viscoelasticity [4], bioengineering [5], control theory [6], electromagnetic theory [7], potential theory [8], electric technology [9], biology [10], industrial robotics [11], mathematical economy [12], plasma physics [13], etc. The real-world processes, which we have to deal with, are generally of fractional order. Heat diffusion into a semi-infinite solid where heat flow equals half-derivative of temperature is an example of a fractional order system.

Differential equations which govern the systems with memory are fractional differential equations (FDEs). The arbitrariness in their order introduces more degrees of freedom in design and analysis, resulting in more accurate modelling, better robustness in control and greater flexibility in signal processing [14]. By this time, it is established that the electrochemical phenomena such as double-layer charge distribution or the diffusion process can be better explained with the fractional-order system. As a result, the modelling of lithium in battery, fuel cells and supercapacitors is carried out with FDEs. The characterisation of ceramic bodies, fractal structures, viscoelastic materials, the decay rate of fruits and meats, the study of corrosion in a metal surface etc. are also promising areas of its applications. Fractional-order system is also a popular choice to study real-time events such as earthquake propagation, volcanic phenomenon, the design of phermokinetics, modelling of human lungs and skin. Even the characteristics of economic market fluctuation adopt fractional calculus-based system modelling. So, the fractional-order analysis has now reached from inert physical network to living network of biology, ecology, physiology and sociology reminding us Leibnitz's prediction in his paper to L'Hopital in 1695 that the fractional differential operator is "an apparent paradox from which one day useful consequences will be drawn".

Bloch equations are a set of first-order macroscopic differential equations. They describe the magnetisation behaviour under static, varying magnetic fields and relaxation. F Bloch introduced these equations in the year 1946 and used them for describing nuclear magnetic resonance (NMR). They are also used in magnetic resonance imaging (MRI) and electron spin resonance (ESR) spectroscopies. Relaxation of the spin system is well described phenomenologically by them, which features the rate of change of magnetisation M of the spin system. An exciting class of complex phenomena arises in NMR spectroscopy and imaging, where the initial point is solving Bloch equations for combinations of gradient magnetic fields and applied static, radiofrequency. MRI is a powerful tool for obtaining spatially localised information from the NMR of atoms within a sample. Bloch equations are given by the following simultaneous system of equations:

$$\left.\begin{aligned} \frac{\mathrm{d}M_x(t)}{\mathrm{d}t} &= \omega_0 M_y(t) - \frac{M_x(t)}{T_2} \\ \frac{\mathrm{d}M_y(t)}{\mathrm{d}t} &= -\omega_0 M_x(t) - \frac{M_y(t)}{T_2} \\ \frac{\mathrm{d}M_z(t)}{\mathrm{d}t} &= \frac{M_0 - M_z(t)}{T_1} \end{aligned}\right\}, \tag{1}$$

with starting conditions $M_x(0) = 0$, $M_y(0) = 100$ and $M_z(0) = 0$.

$M_x(t)$, $M_y(t)$ and $M_z(t)$ show system magnetisation in x, y and z components, respectively. $\omega_0 = 2\pi f_0$ is the frequency of resonance. $B_0 = \omega_0/\gamma$ is the static magnetic field in the z-component. M_0 is the equilibrium magnetisation. T_1 and T_2 are the spin–lattice and spin–spin relaxation times, respectively. This integer-order equation is well posed. Several methods are available in the literature for the approximate solution of the standard Bloch equations [15–18].

The exact solution to eq. (1) is given as

$$\left.\begin{aligned} M_x(t) &= \mathrm{e}^{-t/T_2}\left(M_x(0)\cos w_0 t + M_y(0)\sin w_0 t\right) \\ M_y(t) &= \mathrm{e}^{-t/T_2}\left(M_y(0)\cos w_0 t - M_x(0)\sin w_0 t\right) \\ M_z(t) &= M_z(0)\,\mathrm{e}^{-t/T_1} M_0\left(1 - \mathrm{e}^{-t/T_1}\right) \end{aligned}\right\}. \tag{2}$$

The steady-state solution is found from the asymptotic limit $t \to \infty$ [19]. It is supposed that spins relax in the xy-plane and along the z-axis at diverse rates R_1 and R_2 ($R_i = 1/T_i$, $i = 1, 2$) but follow first-order kinetics. To study the complex structure, heterogeneity and effects of memory in the relaxation process, the standard Bloch equations were generalised to the Bloch equations of fractional order by extending integer order time derivative to Caputo fractional derivative. Fractional Bloch equations were presented in 2008 by Magin *et al* [20] to define a broader range of experimental conditions including porous, heterogeneous or compound materials. These are given as

$$\left.\begin{aligned} \frac{\mathrm{d}^\alpha M_x(t)}{\mathrm{d}t^\alpha} &= \omega_0 M_y(t) - \frac{M_x(t)}{T_2} \\ \frac{\mathrm{d}^\beta M_y(t)}{\mathrm{d}t^\beta} &= -\omega_0 M_x(t) - \frac{M_y(t)}{T_2} \\ \frac{\mathrm{d}^\gamma M_z(t)}{\mathrm{d}t^\gamma} &= \frac{M_0 - M_z(t)}{T_1} \end{aligned}\right\}, \tag{3}$$

subject to conditions $M_x(0) = 0$, $M_y(0) = 100$ and $M_z(0) = 0$.

Here, $0 < \alpha, \beta, \gamma \leq 1$. α, β and γ are orders of time-fractional derivatives. The total order of the system is (α, β, γ). All parameters ω_0, T_1 and T_2 possess units of $s^{-\alpha}$ which keep a consistent set of units for magnetisation. The first and second equations in eq. (3) are coupled while the third one is independent.

A fraction in time derivative suggests weighting of system memory or modulation. The assumption of fractional-order derivatives plays a significant part affecting spin dynamics designated by eq. (3). The physical sense of the above equations goes back to the basic formulation of fractional-order Schrödinger equation in quantum mechanics. It is well known that the fractional derivative is heavily reliant on initial settings and so a suitable fractional derivative must be chosen for handling them. The initial state of the system in NMR is detailed by magnetisation components and so they need to be visibly recognised. Stability of these equations is already investigated and proved in [21]. The mathematical model of fractional Bloch equations is solved by homotopy perturbation method (HPM) [22], predictor–corrector method [23,24], operational matrix method [25–27], implicit alternating direction method [28], Galerkin finite element method [29], etc. The fractional Bloch model has not yet been studied by fractional variation iteration method (FVIM) and fractional homotopy perturbation transform method (FHPTM).

FVIM [30–33] directly attacks the nonlinear FDEs without a need to find certain polynomials for nonlinear terms and gives result in an infinite series that rapidly converges to an analytical solution. This method does not require linearisation, discretisation, little perturbations or any restrictive assumptions. It lessens mathematical computations significantly. Also, FHPTM shows how the transform of Laplace may be applied to approximate the solution of nonlinear FDEs by handling HPM. The perturbation technique [34,35] has many limitations, e.g. the approximate solution contains a succession of small parameters which is troublesome as most nonlinear problems possess no such parameters. FHPTM [36,37] is a neat amalgamation of HPM, the standard transform of Laplace and He's polynomials. The superiority of this scheme is that it has the potential of assimilating two strong computational methodologies for probing nonlinear coupled FDEs.

The aim of this paper is to obtain numerical solution of the time-fractional model of Bloch equations by FVIM, FHPTM and compare our results with those from the existing techniques and with the exact solution. We have used Caputo fractional derivatives because, with these derivatives, initial conditions for FDEs have similar form as for the integer-order differential equations [38].

This paper is structured in the following manner. Section 1 is Introduction. In §2, we give a brief review of the preliminary description of Caputo fractional derivative and some other results, helpful for learning FDEs. In §3, the basic plan of the proposed numerical method FVIM is shown by taking the problem under consideration. In §4, sufficient conditions for the convergence of FVIM and its error estimate are given. Also, FVIM is implemented on a numerical test example to find approximate numerical solution and the conditions for the existence of positive and bounded solution are established. In §5, the basic plan of the hybrid method FHPTM is provided along with its implementation on a numerical test problem. Section 6 deals with the discussion of the obtained numerical results with the help of table and figures. Figures are drawn using the Maple package. In §7, we recapitulate our outcomes and draw inferences.

2. Preliminaries

In this section, we give some basic definitions and properties of fractional calculus.

DEFINITION 2.1

A real function $h(\chi)$, $\chi > 0$ is called in space C_ζ, $\zeta \in R$ if $\ni$ a real number $b(>\zeta)$, s.t. $h(\chi) = \chi^b h_1(\chi)$, $h_1 \in C\,[0,\infty)$. It is clear that $C_\zeta \subset C_\gamma$ if $\gamma \le \zeta$.

DEFINITION 2.2

Consider a function $h(\chi)$, $\chi > 0$. It is called in space C_ζ^m, $m \in \mathbb{N} \cup \{0\}$ if $h^{(m)} \in C_\zeta$.

DEFINITION 2.3

Left-sided Caputo fractional derivative of h, $h \in C_{-1}^m$, $m \in \mathbb{N} \cup \{0\}$,

$$D_t^\beta h\,(t) = \begin{cases} I^{m-\beta} h^{(m)}(t), m-1<\beta<m, m \in \mathbb{N}, \\ \dfrac{\mathrm{d}^m}{\mathrm{d}t^m} h(t),\ \beta = m, \end{cases}$$

a. $I_t^\zeta h(x,t) = \dfrac{1}{\Gamma\zeta} \int_0^t (t-s)^{\zeta-1}\, h(x,s)\,\mathrm{d}s;\ \zeta, t > 0.$

b. $D_\tau^\nu V(x,\tau) = I_\tau^{m-\nu} \dfrac{\partial^m V(x,\tau)}{\partial t^m}$, $m-1 < \nu \le m$.

c. $D_t^\zeta I_t^\zeta h(t) = h(t)\,, m-1 < \zeta \le m, m \in \mathbb{N}$.

d. $I_t^\zeta D_t^\zeta h(t) = h(t) - \sum_{k=1}^{m-1} h^k(0^+) \dfrac{t^k}{k!}$,

$m-1 < \zeta \le m, m \in \mathbb{N}$.

e. $I^\upsilon t^\zeta = \dfrac{\Gamma(\zeta+1)}{\Gamma(\upsilon+\zeta+1)} t^{\upsilon+\zeta}$.

DEFINITION 2.4

The Laplace transform of Caputo fractional derivative is

$$L\big[D^\alpha g(t)\big] = p^\alpha L\,[g(t)] - \sum_{k=0}^{n-1} p^{\alpha-k-1} g^{(k)}\big(0^+\big),$$
$$n-1 < \alpha \le n.$$

Lemma 2.5 [39]. *If u and its partial derivatives are continuous, the fractional derivative* $D_t^\alpha u(x,y,z,t)$ *is bounded.*

3. Basic plan of FVIM for time-fractional Bloch equations

Consider the mathematical model described by eq. (3) as

$$\left.\begin{aligned} \frac{\mathrm{d}^\alpha M_x(t)}{\mathrm{d}t^\alpha} &= \omega_0 M_y(t) - \frac{M_x(t)}{T_2} \\ \frac{\mathrm{d}^\beta M_y(t)}{\mathrm{d}t^\beta} &= -\omega_0 M_x(t) - \frac{M_y(t)}{T_2} \\ \frac{\mathrm{d}^\gamma M_z(t)}{\mathrm{d}t^\gamma} &= \frac{M_0 - M_z(t)}{T_1} \end{aligned}\right\},$$

where $0 < \alpha, \beta, \gamma \le 1$ with initial conditions $M_x(0) = 0$, $M_y(0) = 100$ and $M_z(0) = 0$.

A correction functional is constructed for eq. (3) as

$$\left.\begin{aligned} & M_{x(n+1)}(t) = M_{x(n)} \\ &\quad + \int_0^t \lambda \left(\frac{\mathrm{d}^\alpha M_{x(n)}(t)}{\mathrm{d}\tau^\alpha} - \omega_0 \widetilde{M_{y(n)}}(t) \right. \\ &\quad \left. + \frac{\widetilde{M_{x(n)}}(t)}{T_2} \right) (\mathrm{d}\tau)^\alpha \\ & M_{y(n+1)}(t) = M_{y(n)} \\ &\quad + \int_0^t \lambda \left(\frac{\mathrm{d}^\beta M_{y(n)}(t)}{\mathrm{d}\tau^\beta} + \omega_0 \widetilde{M_{x(n)}}(t) \right. \\ &\quad \left. + \frac{\widetilde{M_{y(n)}}(t)}{T_2} \right) (\mathrm{d}\tau)^\alpha \\ & M_{z(n+1)}(t) = M_{z(n)} \\ &\quad + \int_0^t \lambda \left(\frac{\mathrm{d}^\gamma M_{z(n)}(t)}{\mathrm{d}\tau^\gamma} - \frac{M_0 - \widetilde{M_{z(n)}}(t)}{T_1} \right) (\mathrm{d}\tau)^\alpha \end{aligned}\right\}, \tag{4}$$

where λ is the Lagrangian multiplier.

By variational theory, λ must satisfy

$$\left.\frac{\mathrm{d}^\alpha \lambda}{\mathrm{d}\tau^\alpha}\right|_{\tau=t} = 0 \text{ and } 1+\lambda|_{\tau=t} = 0.$$

We quickly get $\lambda = -1$. Then, using this value in eq. (4), we get

$$\left.\begin{aligned}
M_{x(n+1)}(t) &= M_{x(n)} - \int_0^t \left(\frac{\mathrm{d}^\alpha M_{x(n)}(t)}{\mathrm{d}\tau^\alpha} - \omega_0 M_{y(n)}(t) + \frac{M_{x(n)}(t)}{T_2} \right) (\mathrm{d}\tau)^\alpha \\
M_{y(n+1)}(t) &= M_{y(n)} - \int_0^t \left(\frac{\mathrm{d}^\beta M_{y(n)}(t)}{\mathrm{d}\tau^\beta} + \omega_0 M_{x(n)}(t) + \frac{M_{y(n)}(t)}{T_2} \right) (\mathrm{d}\tau)^\alpha \\
M_{z(n+1)}(t) &= M_{z(n)} - \int_0^t \left(\frac{\mathrm{d}^\gamma M_{z(n)}(t)}{\mathrm{d}\tau^\gamma} - \frac{\left(M_0 - M_{z(n)}(t)\right)}{T_1} \right) (\mathrm{d}\tau)^\alpha
\end{aligned}\right\}. \tag{5}$$

Consecutive approximations $M_{x(n)}(t)$, $M_{y(n)}(t)$ and $M_{z(n)}(t)$, $n \geq 0$ can be built henceforth. $\widetilde{M_{x(n)}}$, $\widetilde{M_{y(n)}}$ and $\widetilde{M_{z(n)}}$ are restricted variations, i.e. $\delta \widetilde{M_{x(n)}} = 0$, $\delta \widetilde{M_{y(n)}} = 0$ and $\delta \widetilde{M_{z(n)}} = 0$. Finally, we get sequences $M_{x(n+1)}(t)$, $M_{y(n+1)}(t)$ and $M_{z(n+1)}(t)$ for $n \geq 0$ of the solution and consequently, exact solution is found as

$$\left.\begin{aligned}
M_x(t) &= \lim_{n\to\infty} M_{x(n)}(t) \\
M_y(t) &= \lim_{n\to\infty} M_{y(n)}(t) \\
M_z(t) &= \lim_{n\to\infty} M_{z(n)}(t)
\end{aligned}\right\}. \tag{6}$$

Algorithm

Step I. Find $u_0 = u(x, 0)$ given by initial approximation, set $n = 0$;
Step II. Use computed values of u_n to obtain u_{n+1} from eq. (5);
Step III. Define $u_n := u_{n+1}$;
Step IV. If $\max|u_{n+1} - u_n| <$ tolerance limit (Tol) stop, otherwise continue;
Step V. Set $u_{n+1}:=u_n$;
Step VI. Set $n = n + 1$, return to Step II.

4. Convergence analysis of FVIM

Now, our emphasis is on the convergence of the proposed FVIM applied to eq. (3) in§3. Sufficient conditions for the convergence of FVIM and its error estimate [40] are provided.

We define the operators B_1, B_2 and B_3 as

$$\left.\begin{aligned}
B_1 &= \int_0^t (-1) \times \left(\frac{\mathrm{d}^\alpha M_{x(n)}(t)}{\mathrm{d}\tau^\alpha} - \omega_0 M_{y(n)}(t) + \frac{M_{x(n)}(t)}{T_2} \right) (\mathrm{d}\tau)^\alpha \\
B_2 &= \int_0^t (-1) \times \left(\frac{\mathrm{d}^\beta M_{y(n)}(t)}{\mathrm{d}\tau^\beta} + \omega_0 M_{x(n)}(t) + \frac{M_{y(n)}(t)}{T_2} \right) (\mathrm{d}\tau)^\alpha \\
B_3 &= \int_0^t (-1) \times \left(\frac{\mathrm{d}^\gamma M_{z(n)}(t)}{\mathrm{d}\tau^\gamma} - \frac{\left(M_0 - M_{z(n)}(t)\right)}{T_1} \right) (\mathrm{d}\tau)^\alpha
\end{aligned}\right\}. \tag{7}$$

Also, we define the components $v_{k(i)}$, $k = 0, 1, 2, \ldots,$ $i = 1, 2, 3$ as

$$\left.\begin{aligned}
M_x(t) &= \lim_{n\to\infty} M_{x(n)}(t) = \sum_{k=0}^{\infty} v_{k(1)} \\
M_y(t) &= \lim_{n\to\infty} M_{y(n)}(t) = \sum_{k=0}^{\infty} v_{k(2)} \\
M_z(t) &= \lim_{n\to\infty} M_{z(n)}(t) = \sum_{k=0}^{\infty} v_{k(3)}
\end{aligned}\right\}. \tag{8}$$

The above solutions in series converge very rapidly.

Theorem 1 [41]. *Let B_1, B_2 and B_3, defined in eq. (7), be operators from Banach space BS to BS. The series solutions as defined in eq. (8) converge if $0 < p < 1$ exists such that*

$$\|B_i[v_{0(i)} + v_{1(i)} + v_{2(i)} + \cdots + v_{k+1(i)}]\| \leq p\|B_i[v_{0(i)} + v_{1(i)} + v_{2(i)} + \cdots + v_{k(i)}]\|, \quad 1 \leq i \leq 3$$

(i.e. $\|v_{k+1}\| \leq p\|v_k\|$), $\forall k \in \mathbb{N} \bigcup \{0\}$.

Theorem 1 is an exceptional case of Banach fixed point theorem used in [42] as sufficient condition to discuss the convergence of FVIM for various differential equations.

Theorem 2 [41]. *If the solution defined in eq. (8) converges, it is an exact solution of problem (3).*

Theorem 3 [41]. *Suppose the series solution (8) converges to solutions $M_x(t)$, $M_y(t)$, and $M_z(t)$ of problem*

(3). *If the truncated series* $\sum_{k=0}^{j} v_{k(1)}$ *is used as an approximation to the solution* $M_x(t)$ *of problem* (3), *then the maximum error* $E_j(t)$ *is assessed as* $E_j(t) \leq (1/(1-p))\, p^{j+1}\|v_0\|$.

If for every $i \in \mathbb{N}\bigcup\{0\}$, *we define the parameters*

$$\chi_i = \begin{cases} \|v_{i+1}\|/\|v_i\|, \ \|v_i\| \neq 0, \\ 0, \ \|v_i\| = 0, \end{cases}$$

then the series solution $\sum_{k=0}^{\infty} v_{k(i)}$, $i = 1, 2, 3$, *of problem* (3) *converges to the exact solution* (8) *when* $0 \leq \chi_i < 1$, $\forall i \in \mathbb{N}\bigcup\{0\}$. *Also, as specified in Theorem* 3, *the maximum absolute truncation error is estimated as* $\|M_x(t) - \sum_{k=0}^{\infty} v_{k(1)}\| \leq (1/(1-\chi))\,\chi^{j+1}\|v_0\|$, *where* $\chi = \max\{\chi_i, i = 0, 1, 2, \ldots, j\}$.

Remark 1 [41]. If first finite χ_i's, $i = 1, 2, \ldots, j$, are not less than 1 and $\chi_i \leq 1$ for $i > j$, then, obviously, the series solution $\sum_{k=0}^{\infty} v_{k(i)}$, $i = 1, 2, 3$, of problem (3) converges to an exact solution. It means that the first finite terms do not affect the convergence of the series solution. Here, the convergence of FVIM depends on χ_i for $i > j$.

4.1 *Numerical implementation of FVIM*

By using conditions, we may initialise with $M_{x0} = 0$, $M_{y0} = 100$ and $M_{z0} = 0$ and using the application of FVIM to eq. (3), we get

$$\left.\begin{aligned} M_{x1}(t) &= M_{x0} - \int_0^t \left(\frac{\mathrm{d}^\alpha M_{x0}(t)}{\mathrm{d}\tau^\alpha} - \omega_0 M_{y0}(t) + \frac{M_{x0}(t)}{T_2} \right) (\mathrm{d}\tau)^\alpha = \frac{100\omega_0 t^\alpha}{\Gamma(1+\alpha)} \\ M_{y1}(t) &= M_{y0} - \int_0^t \left(\frac{\mathrm{d}^\beta M_{y0}(t)}{\mathrm{d}\tau^\beta} + \omega_0 M_{x0}(t) + \frac{M_{y0}(t)}{T_2} \right) (\mathrm{d}\tau)^\beta = 100 - \frac{100\, t^\beta}{T_2\Gamma(1+\beta)} \end{aligned}\right\}, \tag{9}$$

$$M_{z1}(t) = M_{z0} - \int_0^t \left(\frac{\mathrm{d}^\gamma M_{z0}(t)}{\mathrm{d}\tau^\gamma} - \frac{(M_0 - M_{z0}(t))}{T_1} \right) (\mathrm{d}\tau)^\gamma = \frac{M_0 t^\gamma}{T_1\Gamma(1+\gamma)},$$

$$\left.\begin{aligned} M_{x2}(t) &= \frac{100\omega_0 t^\alpha}{\Gamma(1+\alpha)} - \frac{100\omega_0 t^{2\alpha}}{T_2\Gamma(1+2\alpha)} - \frac{100\omega_0 t^{\alpha+\beta}}{T_2\Gamma(1+\alpha+\beta)} \\ M_{y2}(t) &= 100 - \frac{100 t^\beta}{T_2\Gamma(1+\beta)} - \frac{100\omega_0^2 t^{\alpha+\beta}}{\Gamma(1+\alpha+\beta)} + \frac{100 t^{2\beta}}{T_2^2\Gamma(1+2\beta)} \\ M_{z2}(t) &= \frac{M_0 t^\gamma}{T_1\Gamma(1+\gamma)} - \frac{M_0 t^{2\gamma}}{T_1^2\Gamma(1+2\gamma)} \end{aligned}\right\}. \tag{10}$$

Proceeding in this way, next iteration components can be found with the help of the Maple package. At last, we can get a solution as

$$\left.\begin{aligned} M_x(t) &= \lim_{n\to\infty} M_{x(n)}(t) \\ M_y(t) &= \lim_{n\to\infty} M_{y(n)}(t) \\ M_z(t) &= \lim_{n\to\infty} M_{z(n)}(t) \end{aligned}\right\}. \tag{11}$$

When $\alpha = \beta = \gamma = 1$, the exact solution of eq. (3) is

$$\left.\begin{aligned} M_x(t) &= \mathrm{e}^{-t/T_2}\big(M_x(0)\cos\omega_0 t + M_y(0)\sin\omega_0 t\big) \\ M_y(t) &= \mathrm{e}^{-t/T_2}\big(M_y(0)\cos\omega_0 t - M_x(0)\sin\omega_0 t\big) \\ M_z(t) &= M_z(0)\,\mathrm{e}^{-t/T_1} M_0\big(1 - \mathrm{e}^{-t/T_1}\big) \end{aligned}\right\}. \tag{12}$$

Considering eqs (7) and (8), iteration formula for problem (3) can be created as

$$v_{0(1)} = 0, \quad v_{0(2)} = 100, \quad v_{0(3)} = 0,$$

$$v_{1(1)} = \frac{100\omega_0 t^\alpha}{\Gamma(1+\alpha)}, \quad v_{1(2)} = -\frac{100\, t^\beta}{T_2\Gamma(1+\beta)},$$

$$v_{1(3)} = \frac{M_0 t^\gamma}{T_1\Gamma(1+\gamma)},$$

$$v_{2(1)} = -\frac{100\omega_0 t^{2\alpha}}{T_2\Gamma(1+2\alpha)} - \frac{100\omega_0 t^{\alpha+\beta}}{T_2\Gamma(1+\alpha+\beta)},$$

$$v_{2(2)} = -\frac{100\omega_0^2 t^{\alpha+\beta}}{\Gamma(1+\alpha+\beta)} + \frac{100\, t^{2\beta}}{T_2^2\Gamma(1+2\beta)},$$

$$v_{2(3)} = -\frac{M_0 t^{2\gamma}}{\mathrm{T}_1^2\Gamma(1+2\gamma)},$$

and so on.

If we compute χ_i's for this problem, we obtain

$$\chi_{i(1)} = \frac{\|v_{i+1(1)}\|}{\|v_{i(1)}\|} = \left\| \frac{-\Gamma(1+i\alpha)}{T_2} \times \left(\frac{t^\alpha}{\Gamma(1+(i+1)\alpha)} + \frac{t^\beta}{\Gamma(1+i(\alpha+\beta))} \right) \right\| < 1,$$

$$\chi_{i(2)} = \frac{\|v_{i+1(2)}\|}{\|v_{i(2)}\|} = \|T_2\Gamma(1+i\beta) \times \left(\frac{\omega_0^2 t^\alpha}{\Gamma(1+i(\alpha+\beta))} - \frac{t^\beta}{T_2^2\Gamma(1+(i+1)\beta)}\right)\Bigg\| < 1,$$

$$\chi_{i(3)} = \frac{\|v_{i+1(3)}\|}{\|v_{i(3)}\|} = \left\|\frac{-\Gamma(1+i\gamma)}{T_1\Gamma(1+(i+1)\gamma)}t^\gamma\right\| < 1.$$

For example, $i \geq 1, 0 < t \leq 1$ and $0 < \alpha, \beta, \gamma \leq 1$. It confirms that the variational approach for problem (3) gives a positive and bounded solution that converges to the exact solution.

Remark 2 [41]. The above test problem is taken when $0 < t \leq 1$ so as to discuss the convergence condition. Certainly, we may stretch the interval and then examine the convergence condition after ignoring the first few terms of the series solution. For example, if we take time-fractional Bloch equations (3) when $0 < t \leq a$ and $\alpha = \beta = \gamma = 1$, where $a > 0$, then

$$\begin{aligned}\chi_{i(1)} &= \left\|\frac{-\Gamma(1+i)}{T_2}\left(\frac{t}{\Gamma(1+(i+1))} + \frac{t}{\Gamma(1+2i)}\right)\right\| \\ &= \left\|\frac{-(i!)}{T_2}\left(\frac{1}{(i+1)!} + \frac{1}{(2i)!}\right)t\right\| \\ &\leq \frac{a}{T_2}\left(\frac{1}{i+1} + \frac{1}{2}\right) < 1, \quad \text{for } i > a,\end{aligned}$$

$$\begin{aligned}\chi_{i(2)} &= \left\|T_2\Gamma(1+i)\left(\frac{\omega_0^2 t}{\Gamma(1+2i)} - \frac{t}{T_2^2\Gamma(1+(i+1))}\right)\right\| \\ &= \left\|T_2 i!\left(\frac{\omega_0^2}{(2i)!} - \frac{1}{T_2^2(i+1)!}\right)t\right\| \\ &\leq aT_2\left(\frac{\omega_0^2}{2} - \frac{1}{T_2^2(i+1)}\right) < 1, \quad \text{for } i > a,\end{aligned}$$

$$\begin{aligned}\chi_{i(3)} &= \left\|t\frac{-\Gamma(1+i)}{T_1\Gamma(1+(i+1))}\right\| \\ &= \left\|t\frac{-(i!)}{T_1(i+1)!}\right\| \leq \frac{a}{T_1(i+1)} < 1, \quad \text{for } i > a.\end{aligned}$$

Hence, the series solution $\sum_{k=0}^{\infty} v_{k(i)}$ is positive, bounded and it converges to exact solution for all $a > 0$.

5. Basic plan of FHPTM for time-fractional Bloch equations

To illustrate the process of the solution by FHPTM, consider the model described by

$$\left.\begin{aligned}\frac{\mathrm{d}^\alpha M_x(t)}{\mathrm{d}t^\alpha} + S_1(u,v) + Q_1(u,v) = g_1(t) \\ \frac{\mathrm{d}^\beta M_y(t)}{\mathrm{d}t^\beta} + S_2(u,v) + Q_2(u,v) = g_2(t) \\ \frac{\mathrm{d}^\gamma M_z(t)}{\mathrm{d}t^\gamma} + S_3(u,v) + Q_3(u,v) = g_3(t)\end{aligned}\right\}, \quad (13)$$

with initial conditions $M_x(0) = 0$, $M_y(0) = 100$ and $M_z(0) = 0$. Here, $\mathrm{d}^\alpha/\mathrm{d}t^\alpha$, $\mathrm{d}^\beta/\mathrm{d}t^\beta$ and $\mathrm{d}^\gamma/\mathrm{d}t^\gamma$ are Caputo fractional operators of order α, β and γ, respectively. g_1, g_2 and g_3 are source terms. S_1, S_2, S_3 and Q_1, Q_2, Q_3 are linear and nonlinear operators, respectively. Also, $0 < \alpha, \beta, \gamma \leq 1$.

The method comprises taking transform of Laplace on both sides of eq. (13) and using differentiation property as

$$\left.\begin{aligned}&L[M_x(t)] = -p^{-\alpha}L[g_1(t)] \\ &\quad + p^{-\alpha}L\left[S_1(M_x, M_y, M_z) + Q_1(M_x, M_y, M_z)\right] \\ &L[M_y(t)] = -p^{-\beta}L[g_2(t)] \\ &\quad + p^{-\beta}L\left[S_2(M_x, M_y, M_z) + Q_2(M_x, M_y, M_z)\right] \\ &L[M_z(t)] = -p^{-\gamma}L[g_3(t)] \\ &\quad + p^{-\gamma}L\left[S_3(M_x, M_y, M_z) + Q_3(M_x, M_y, M_z)\right]\end{aligned}\right\}, \quad (14)$$

Taking the inverse Laplace transform, we get

$$\left.\begin{aligned}M_x(t) &= G_1(t) + L^{-1}\left[p^{-\alpha}L\left\{S_1(M_x, M_y, M_z) + Q_1(M_x, M_y, M_z)\right\}\right] \\ M_y(t) &= G_2(t) + L^{-1}\left[p^{-\beta}L\left\{S_2(M_x, M_y, M_z) + Q_2(M_x, M_y, M_z)\right\}\right] \\ M_z(t) &= G_3(t) + L^{-1}\left[p^{-\gamma}L\left\{S_3(M_x, M_y, M_z) + Q_3(M_x, M_y, M_z)\right\}\right]\end{aligned}\right\}. \quad (15)$$

Here $G_1(t)$, $G_2(t)$ and $G_3(t)$ are the terms obtained from the source term and the given initial values.

Applying the HPM, it is assumed that the result may be articulated as a power series:

$$\left.\begin{aligned}M_x(t) &= \sum_{n=0}^{\infty} p^n M_{xn}(t) \\ M_y(t) &= \sum_{n=0}^{\infty} p^n M_{yn}(t) \\ M_z(t) &= \sum_{n=0}^{\infty} p^n M_{zn}(t)\end{aligned}\right\}. \quad (16)$$

Here, $p \in [0, 1]$ is reflected as a small parameter called homotopy parameter.

The nonlinear terms are decomposed as

$$\left.\begin{aligned} NM_x(t) &= \sum_{n=0}^{\infty} p^n H_n(M_x) \\ NM_y(t) &= \sum_{n=0}^{\infty} p^n H'_n(M_y) \\ NM_z(t) &= \sum_{n=0}^{\infty} p^n H''_n(M_z) \end{aligned}\right\}. \tag{17}$$

where H_n, H'_n and H''_n are He's polynomials of M_{x0}, M_{x1}, M_{x2}, $\dots$, M_{xn}; M_{y0}, M_{y1}, M_{y2}, $\dots$, M_{yn} and M_{z0}, M_{z1}, M_{z2}, $\dots$, M_{zn}, respectively.

They are calculated by the given formulae:

$$\left.\begin{aligned} & H_n(M_{x0}, M_{x1}, M_{x2}, \dots, M_{xn}) \\ &\quad = \frac{1}{n!}\frac{\partial^n}{\partial p^n}\left[N\left(\sum_{i=0}^{\infty} p^i M_{x_i}\right)\right]_{p=0}, n = 0, 1, 2, 3, \dots \\ & H'_n(M_{y0}, M_{y1}, M_{y2}, \dots, M_{yn}) \\ &\quad = \frac{1}{n!}\frac{\partial^n}{\partial p^n}\left[N\left(\sum_{i=0}^{\infty} p^i M_{y_i}\right)\right]_{p=0}, n = 0, 1, 2, 3, \dots \\ & H''_n(M_{z0}, M_{z1}, M_{z2}, \dots, M_{zn}) \\ &\quad = \frac{1}{n!}\frac{\partial^n}{\partial p^n}\left[N\left(\sum_{i=0}^{\infty} p^i M_{z_i}\right)\right]_{p=0}, n = 0, 1, 2, 3, \dots \end{aligned}\right\}. \tag{18}$$

Using eqs (16) and (17) in eq. (15) and applying HPM, we get

$$\begin{aligned} & \sum_{n=0}^{\infty} p^n M_{xn}(t) \\ &\quad = G_1(t) + pL^{-1}\left[p^{-\alpha}L\left\{S_1(M_x, M_y, M_z) + Q_1(M_x, M_y, M_z)\right\}\right], \\ & \sum_{n=0}^{\infty} p^n M_{yn}(t) \\ &\quad = G_2(t) + pL^{-1}\left[p^{-\beta}L\left\{S_2(M_x, M_y, M_z) + Q_2(M_x, M_y, M_z)\right\}\right], \\ & \sum_{n=0}^{\infty} p^n M_{zn}(t) \\ &\quad = G_3(t) + pL^{-1}\left[p^{-\gamma}L\left\{S_3(M_x, M_y, M_z) + Q_3(M_x, M_y, M_z)\right\}\right]. \end{aligned} \tag{19}$$

This is a pairing of HPM and transform of Laplace using He's polynomials. Equating coefficients of the identical powers on both sides, we get

$$\left.\begin{aligned} & p^0: M_{x0}(t) = G_1(t); \quad M_{y0}(t) = G_2(t); \\ & M_{z0}(t) = G_3(t), \\ & p^n: M_{xn}(t) \\ &\quad = L^{-1}\left[p^{-\alpha}L\left\{S_1(M_{xn-1}, M_{yn-1}, M_{zn-1}) + H_{n-1}(M_x, M_y, M_z)\right\}\right], n > 0, n \in \mathbb{N} \end{aligned}\right\}$$

$$M_{yn}(t) = L^{-1}\left[p^{-\beta}L\left\{S_2(M_{xn-1}, M_{yn-1}, M_{zn-1}) + H'_{n-1}(M_x, M_y, M_z)\right\}\right], n > 0, n \in \mathbb{N},$$

$$M_{zn}(t) = L^{-1}\left[p^{-\gamma}L\left\{S_3(M_{xn-1}, M_{yn-1}, M_{zn-1}) + H''_{n-1}(M_x, M_y, M_z)\right\}\right], n > 0, n \in \mathbb{N}.$$

Continuing in this way, the enduring components can completely be achieved also. Thus, the series solution is fully calculated. At last, the analytical solution is approximated by the series

$$\left.\begin{aligned} M_x(t) &= \lim_{p\to 1}\sum_{n=0}^{\infty} p^n M_{xn}(t) \\ M_y(t) &= \lim_{p\to 1}\sum_{n=0}^{\infty} p^n M_{yn}(t) \\ M_z(t) &= \lim_{p\to 1}\sum_{n=0}^{\infty} p^n M_{zn}(t) \end{aligned}\right\}. \tag{20}$$

The above solutions in series converge rapidly.

5.1 *Numerical implementation of FHPTM*

Now, we shall apply FHPTM to a test problem to illustrate its applicability and efficiency. Taking transform of Laplace on both sides of eq. (3), we get

$$\left.\begin{aligned} M_x(p) &= p^{-\alpha}L\left[\omega_0 M_y(t) - \frac{M_x(t)}{T_2}\right] \\ M_y(p) &= 100 + p^{-\beta}L\left[-\omega_0 M_x(t) - \frac{M_y(t)}{T_2}\right] \\ M_z(p) &= p^{-\gamma}L\left[\frac{M_0 - M_z(t)}{T_1}\right] \end{aligned}\right\}. \tag{21}$$

Taking the inverse Laplace transform, we get

$$\left.\begin{aligned} & M_x(t) = L^{-1}\left[p^{-\alpha}L\left\{\omega_0 M_y(t) - \frac{M_x(t)}{T_2}\right\}\right] \\ & M_y(p) \\ &\quad = 100 + L^{-1}\left[p^{-\beta}L\left\{-\omega_0 M_x(t) - \frac{M_y(t)}{T_2}\right\}\right] \\ & M_z(p) = L^{-1}\left[p^{-\gamma}L\left\{\frac{M_0 - M_z(t)}{T_1}\right\}\right] \end{aligned}\right\}. \tag{22}$$

Applying the HPM, we get

$$\left.\begin{aligned} &\sum_{n=0}^{\infty} p^n M_{xn}(t) \\ &\quad = L^{-1}\left[p^{-\alpha} L\left\{\omega_0 M_y(t) - \frac{M_x(t)}{T_2}\right\}\right] \\ &\sum_{n=0}^{\infty} p^n M_{yn}(t) \\ &\quad = 100 + L^{-1}\left[p^{-\beta} L\left\{-\omega_0 M_x(t) - \frac{M_y(t)}{T_2}\right\}\right] \\ &\sum_{n=0}^{\infty} p^n M_{zn}(t) = L^{-1}\left[p^{-\gamma} L\left\{\frac{M_0 - M_z(t)}{T_1}\right\}\right] \end{aligned}\right\}. \tag{23}$$

By equating coefficients of like powers of p on both flanks of eqs (23), we get

$$p^0 : M_{x0} = 0, \quad M_{y0} = 100, \quad M_{z0} = 0.$$

$$p : M_{x1} = \frac{100\omega_0\, t^{\alpha}}{\Gamma(1+\alpha)}, \quad M_{y1} = -\frac{100\, t^{\beta}}{T_2\Gamma(1+\beta)},$$

$$M_{z1} = \frac{M_0 t^{\gamma}}{T_1\Gamma(1+\gamma)}.$$

$$p^2 : M_{x2} = -\frac{100\omega_0 t^{2\alpha}}{T_2\Gamma(1+2\alpha)} - \frac{100\omega_0 t^{\alpha+\beta}}{T_2\Gamma(1+\alpha+\beta)}.$$

$$M_{y2} = -\frac{100\omega_0^2 t^{\alpha+\beta}}{\Gamma(1+\alpha+\beta)} + \frac{100\, t^{2\beta}}{T_2^2\Gamma(1+2\beta)}.$$

$$M_{z2} = \frac{M_0 t^{\gamma}}{T_1\Gamma(1+\gamma)} - \frac{M_0 t^{2\gamma}}{T_1^2\Gamma(1+2\gamma)}$$

and so on.

In this way, the rest components of the FHPTM solution can easily be found.

Thus, the solution is obtained as

$$\left.\begin{aligned} M_x(t) &= \lim_{p\to 1}\sum_{n=0}^{\infty} p^n M_{xn}(t) \\ M_y(t) &= \lim_{p\to 1}\sum_{n=0}^{\infty} p^n M_{yn}(t) \\ M_z(t) &= \lim_{p\to 1}\sum_{n=0}^{\infty} p^n M_{zn}(t) \end{aligned}\right\}. \tag{24}$$

6. Numerical results and discussion

Table 1 shows the comparison of the values of $M_x(t)$, $M_y(t)$ and $M_z(t)$ at $\alpha = 1, t = 0.1$, 0.3, 0.5, 0.7 and 0.9 found by the proposed methods FVIM, FHPTM with the exact solution and those from some existing methods. Numerical results show that our proposed FVIM performs very well for the solution of fractional-order Bloch equations among other existing methods, even when it is used with a lower-order approximate solution. The accuracy can, however, be improved by using higher-order approximate solutions. Figures 1–3 respectively depict the behaviour of exact solution $M_x(t), M_y(t)$ and $M_z(t)$ vs. t at $\alpha = \beta = \gamma = 1$ and its comparison with the numerical solution obtained by using FVIM and FHPTM. It is clear from figures 1 and 2 that the approximate solutions $M_x(t)$ and $M_y(t)$ of fractional Bloch equations, obtained by using FVIM, are in complete agreement with the exact solution in comparison to those by the hybrid method FHPTM. However, in figure 3, the approximate solution $M_z(t)$ by FVIM and FHPTM is in complete agreement with the exact solution. The numerical results for

Table 1. Comparison of approximate solutions by the existing and proposed methods with the exact solution.

M	t	Exact solution	FVIM solution	FHPTM solution	Operational matrix method solution [27]	HPM solution [22]	Iterative method solution [21]
$M_x(t)$	0.1	9.9335	9.9335	9.95256	9.9245	9.9335	9.2237
	0.3	29.1120	29.1120	29.6219	29.1080	29.1034	29.0937
	0.5	46.7588	46.7589	49.0948	46.7732	46.6823	46.7507
	0.7	62.2060	62.2074	68.5244	62.2180	61.8762	62.1921
	0.9	74.8859	74.8943	88.0717	74.8814	73.8911	74.8806
$M_y(t)$	0.1	99.0042	99.0042	99.0037	99.0213	99.0187	99.0051
	0.3	94.1113	94.1113	94.0731	94.1645	94.1837	94.1166
	0.5	85.5915	85.5914	85.2988	85.5689	85.5518	85.5942
	0.7	73.8536	73.8529	72.7400	73.7886	73.1630	73.8635
	0.9	59.4258	59.4215	56.4183	59.3782	57.0572	59.4296
$M_z(t)$	0.1	0.0952	0.0952	0.0952	0.0952	0.0952	0.0952
	0.3	0.2592	0.2592	0.2592	0.2592	0.2592	0.2590
	0.5	0.3935	0.3935	0.3935	0.3935	0.3935	0.3934
	0.7	0.5034	0.5034	0.5034	0.5034	0.5034	0.5033
	0.9	0.5934	0.5934	0.5934	0.5934	0.5934	0.5934

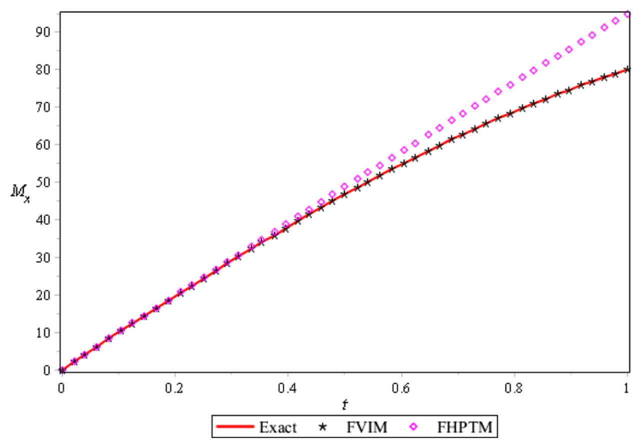

Figure 1. Behaviour of the exact solution $M_x(t)$ vs. t and its comparison with an approximate solution by FVIM and FHPTM at $\alpha = 1$.

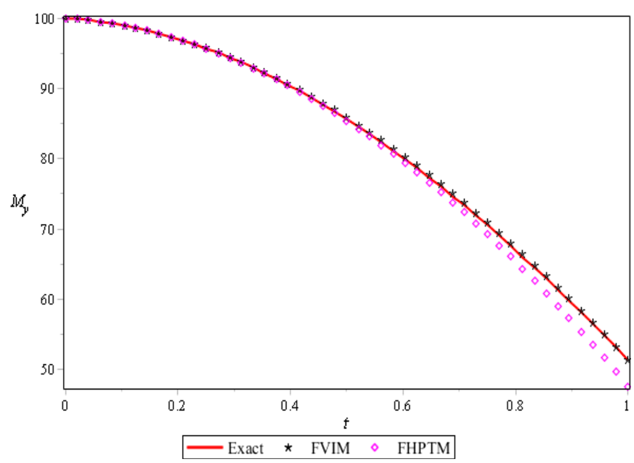

Figure 2. Behaviour of exact solution $M_y(t)$ vs. t and its comparison with an approximate solution by FVIM and FHPTM at $\beta = 1$.

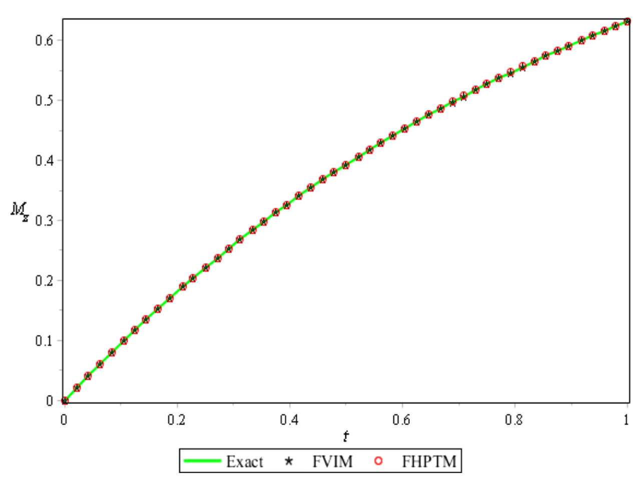

Figure 3. Behaviour of the exact solution $M_z(t)$ vs. t and its comparison with an approximate solution by FVIM and FHPTM at $\gamma = 1$.

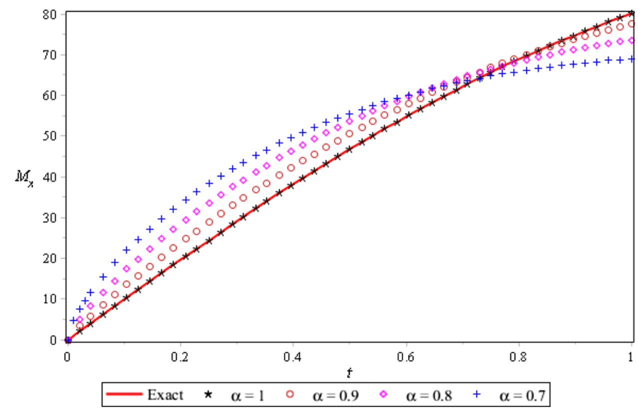

Figure 4. Comparison of an approximate solution $M_x(t)$ at different values of α by FVIM and exact solution at $\alpha = 1$.

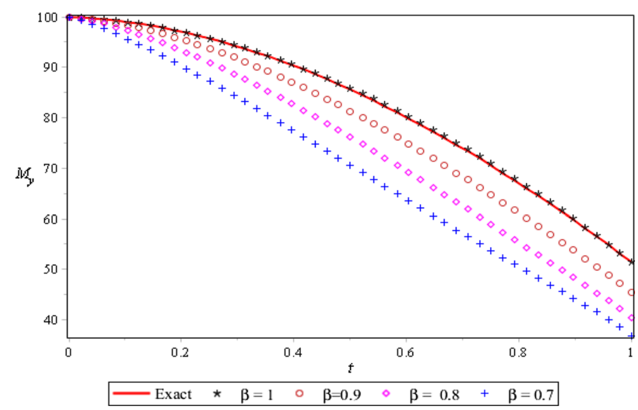

Figure 5. Comparison of an approximate solution $M_y(t)$ at different values of β by FVIM and exact solution at $\beta = 1$.

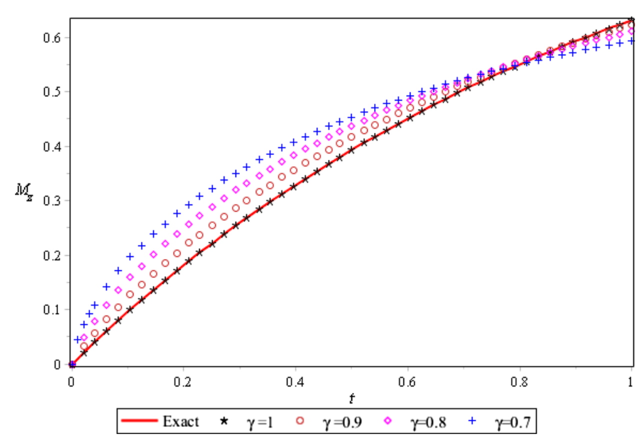

Figure 6. Comparison of an approximate solution $M_z(t)$ at different values of γ by FVIM and exact solution at $\gamma = 1$.

different specific cases of α, β and γ are presented in figures 4–6. In figures 4 and 6, it is clear that $M_x(t)$ and $M_z(t)$ increase with increase in time t for $\alpha = \gamma = 0.7, 0.8, 0.9$ and converges to the exact solution at $\alpha = \gamma = 1$, while in figure 5, $M_y(t)$ decreases with increase in time t for $\beta = 0.7, 0.8$ and 0.9, but again converges to the exact solution at $\beta = 1$.

7. Conclusions

In this paper, FVIM and FHPTM are successfully applied to solve the fractional model of Bloch equations. It is apparently seen from the illustrative example that FVIM is easy to implement and is a powerful numerical method to find an approximate solution compared to FHPTM and other existing methods. It is also shown by convergence analysis that the numerical solution obtained by FVIM is positive, bounded and converges to the exact solution. It should be noted that FVIM is used directly without using linearisation, perturbation, Adomian polynomials or any other restrictive assumptions. The results of fractional Bloch equations by FVIM are much closer to the exact solutions compared to those obtained by the existing hybrid techniques. Hence, FVIM is more efficient, convenient and easier than other existing methods.

Acknowledgements

The authors are thankful to the anonymous reviewers and editors for their valuable comments and suggestions to improve the quality of this paper.

References

[1] J H He, *Bull. Sci. Technol. Soc.* **15**(**2**), 86 (1999)
[2] A D Robinson, *Annu. Rev. Neurosci.* **4**, 463 (1981)
[3] M Mirzazadeh, *Pramana – J. Phys.* **86**(**5**), 957 (2016)
[4] R L Bagley and P J Torvik, *AIAA J.* **23**(**6**), 918 (1985)
[5] R L Magin, *Crit. Rev. Biomed. Eng.* **32**(**1**), 1 (2004)
[6] G W Bohannan, *J. Vib. Control* **14**(**9–10**), 1487 (2008)
[7] N Engheia, *IEEE Antennas Propag. Mag.* **39**(**4**), 35 (1997)
[8] G Cooper and D Cowan, *Explor. Geophys.* **34**(**1/2**), 51 (2003)
[9] M F Ali, M Sharma and R Jain, *Adv. Eng. Tech. Appl.* **5**(**2**), 41 (2016)
[10] R L Magin, *Comput. Math. Appl.* **59**(**5**), 1586 (2010)
[11] Q Xu, J Huang and L Zhou, *Proceedings of the 34th Chinese Control Conference* (2015) p. 4501
[12] H Fallahgoul, S Focardi and F Fabozzi, *Fractional calculus and fractional processes with applications to financial economics* (Academic Press, San Diego, 2016)
[13] Y W Zhang, *Pramana – J. Phys.* **90**, 34 (2018)
[14] R Panda and M Dash, *Signal Process.* **86**(**9**), 2340 (2006)
[15] O B Awojoyogber, *Phys. A: Stat. Mech. Appl.* **339**(**3–4**), 437 (2004)
[16] K Murase and N Tanki, *Magn. Reson. Imaging* **29**(**1**), 126 (2011)
[17] S Balac and L Chupin, *Math. Comput. Model.* **48**(**11–12**), 1901 (2008)
[18] J C Leyte, *Chem. Phys. Lett.* **165**(**2–3**), 213 (1990)
[19] D Matignon, *IMACS – SMC Proceedings* (Lille, France, 1996) p. 963
[20] R L Magin, O Abdullah, D Baleanu and X Zhou, *J. Magn. Reson.* **190**(**2**), 255 (2008)
[21] I Petráš, *Comput. Math. Appl.* **61**(**2**), 341 (2011)
[22] S Kumar, N Faraz and K Sayevand, *Walailak J. Sci. Tech.* **11**(**4**), 273 (2014)
[23] Q Yu, F Liu, I Turner and K Burrage, *J. Comput. Appl. Math.* **255**, 635 (2014)
[24] S Qin, F Liu, I Turner, V Vegh and Q Yu, *J. Comput. Appl. Math.* **319**, 308 (2017)
[25] H Singh, *Alexandria Eng. J.* **55**(**3**), 2863 (2016)
[26] H Singh and C S Singh, *Alexandria Eng. J.* (in press), https://doi.org/10.1016/j.aej.2017.07.002 (2017)
[27] H Singh, *J. King Saud Univ. Eng. Sci.* **29**(**2**), 235 (2017)
[28] S Qin, F Liu, I W Turner, Q Yang and Q Yu, *Comput. Math. Appl.* **75**(**1**), 7 (2018)
[29] Y Zhao, W Bu, X Zhao and Y Tang, *J. Comput. Phys.* **350**, 117 (2017)
[30] J H He, *Int. J. Nonlinear Mech.* **34**(**4**), 699 (1999)
[31] A Prakash and M Kumar, *J. Appl. Anal. Comput.* **6**(**3**), 738 (2016)
[32] J H He and X H Wu, *Comput. Math. Appl.* **54**(**7–8**), 881 (2007)
[33] A Prakash, M Kumar and K K Sharma, *Appl. Math. Comput.* **260**, 314 (2015)
[34] J H He, *Comput. Method. Appl. M.* **178**(**3–4**), 257 (1999)
[35] J H He, *Int. J. Nonlinear Mech.* **35**(**1**), 37 (2000)
[36] A Prakash, *Nonlinear Eng.* **5**(**2**), 123 (2016)
[37] S Kumar, *Appl. Math. Model.* **38**(**13**), 3154 (2014)
[38] I Podlubny, *Fractional differential equations* (Academic Press, New York, 1999)
[39] A A Elbeleze, A Kiliçman and B M Taib, *Abstr. Appl. Anal.* **2014**, 518343 (2014)
[40] M G Sakar and H Ergoren, *Appl. Math. Model.* **39**(**14**), 3972 (2015)
[41] Z M Odibat, *Math. Comput. Model.* **51**(**9–10**), 1181 (2010)
[42] M Tatari and M Dehghan, *J. Comput. Appl. Math.* **207**(**1**), 121 (2007)